J. For. Res. (2018) 29(5):1215–1224
https://doi.org/10.1007/s11676-017-0540-2

ORIGINAL PAPER

Comparable water use of two contrasting riparian forests in the lower Heihe River basin, Northwest China

Tengfei Yu[1,2,3] · Qi Feng[1,2,3] · Jianhua Si[1,2,3] · Xiaoyou Zhang[1,2] · Haiyang Xi[1,2,3] · Chunyan Zhao[1]

Received: 11 August 2016 / Accepted: 16 November 2016 / Published online: 15 November 2017

Abstract Understanding forest ecosystem evapotranspiration (*ET*) is crucial for water-limited environments, particularly those that lack adequate quantified data such as the lower Heihe River basin of northwest China which is primarily dominated by *Tamarix ramosissima* Ledeb. and *Populus euphratica* Oliv. forests. Accordingly, we selected the growing season for 2 years (2012 and 2014) of two such forests under similar meteorological conditions to compare *ET* using the eddy covariance (EC) technique. During the growing seasons, daily *ET* of *T. ramosissima* ranged from 0.3 to 8.0 mm day^{-1} with a mean of 3.6 mm day^{-1}, and daily *ET* of *P. euphratica* ranged from 0.9 to 7.9 mm day^{-1} with a mean of 4.6 mm day^{-1} for a total of 548 and 707 mm, respectively. The significantly higher *ET* of the *P. euphratica* stand was directly linked to high soil evaporation rates under sufficient water availability from irrigation. When the soil evaporation was disregarded, water use was comparable to two contrasting riparian forests, a *P. euphratica* forest with a total transpiration of 465 mm and a *T. ramosissima* forest with 473 mm. Regression analysis demonstrated that climate factors accounted for at least 80% of *ET* variation in both forest types. In conclusion, water use of the riparian forests was low and comparable in this arid region, that suggest the long-term plant adaptation to the local climate and conditions of water availability.

Keywords Eddy covariance · Evapotranspiration · Heihe River basin · Riparian forest

Introduction

Evapotranspiration (*ET*) is a major component of catchment water balances. Because *ET* in most large basin ecosystems is limited by rainfall, riparian corridors are hot spots for atmospheric water loss for large arid- and semi-arid basins (Sala et al. 1996; Smith et al. 1998). In the lower Heihe River basin (HRB), northwestern China, riparian forests are dominated by phreatophytes, such as *Populus euphratica* Oliv. tree species and *Tamarix ramosissima* Ledeb. shrub species (Si et al. 2007). Phreatophytes are deep-rooted plants that obtain their water from the water table or the soil above it. Over the past several decades, the eco-environment of riparian forests has markedly deteriorated to the extent that riparian forests have decreased in size and their ecological functions have declined (Cheng et al. 2014; Feng and Cheng 1998; Si et al. 2007). In order to restore riparian forests in the lower HRB, the Ecological Water Conveyance Project (EWCP) was initiated in 2000 by the government of China to recharge

Project funding: This study was supported by the National Natural Science Foundation of China (41401033, 31370466, and 41271037), the China Postdoctoral Science Foundation (2014M560819) and the National Key Research and Development Program of China (2016YFC0501002).

The online version is available at http://www.springerlink.com

Corresponding editor: Hu Yanbo.

✉ Qi Feng
qifeng@lzb.ac.cn

[1] Alxa Desert Eco-hydrology Experimental Research Station, Northwest Institute of Eco-Environment and Resources, Chinese Academy of Sciences, Lanzhou 730000, China

[2] Key Laboratory of Eco-hydrology of Inland River Basin, Chinese Academy of Sciences, Lanzhou 730000, China

[3] Gansu Hydrology and Water Resources Engineering Research Center, Lanzhou 730000, China

Table 1 Mean values ± SD of meteorological variables, including total precipitation (*P*, mm), mean daylight hours (*N*, h), air temperature (T_a, °C), relative humidity (*RH*, %), saturated vapor pressure deficit (*VPD*, kPa), and wind speed (*U*, m s^{-1}) from the Ejin meteorological station for the years 2012 and 2014

Year	*P* (mm)	*N* (h)	T_a (°C)	*RH* (%)	*VPD* (kPa)	*U* (m s^{-1})
2012	32.7	8.77 ± 3.04	9.44 ± 14.47	27.72 ± 12.23	1.39 ± 1.05	2.60 ± 1.09
2014	17.2	8.33 ± 3.15	10.55 ± 13.30	30.16 ± 12.14	1.38 ± 1.10	2.63 ± 1.11
Sig.		No	No	Yes	No	No

Significant differences were tested using one-way ANOVA at $P = 0.05$

water back into the lower HRB (Guo et al. 2008). Although *P. euphratica* forests were maintained after this water conveyance program was put into practice (from 295.69 km^2 in 1982 to 294.30 km^2 in 2010), *T. ramosissima* forests have expanded in area (from 1003.71 km^2 in 1982 to 1529.56 km^2 in 2010). Accordingly, it is important to quantify water consumption by these two forest types in order to effectively utilize their limited water resources.

Although *P. euphratica* is an important structural tree species of riparian forests, only a limited number of *ET* studies have been conducted in this region. Studies mainly focused on a tree-level scale (Si et al. 2007; Zhang et al. 2006) and rarely on a stand-level scale (Hou et al. 2010). Annual transpiration measured through sap flow was 214.9 mm (Si et al. 2007), less than the total *ET* (447.0 mm) estimated by the Bowen ratio energy balance (BREB) method at the same site (Hou et al. 2010). In addition, *T. ramosissima* is a native phreatophytic that originates from arid regions in Central Asia, and has widely invaded numerous western states (Di Tomaso 1998; Hatler and Hart 2009; Shafroth et al. 2005). Generally, *T. ramosissima* is recognized as a prolific water user. Data taken from flux towers (Cleverly et al. 2002, 2006; Devitt et al. 1998) and large area estimates using remote sensing techniques (Bawazir et al. 2009; Dennison et al. 2009; Nagler et al. 2009) have yielded moderate water use rates (from 800 to 1450 mm $year^{-1}$). In contrast to the western U.S., *ET* from *T. ramosissima* stands was approximately 500 mm $year^{-1}$ in the lower Tarim River basin (Yuan et al. 2014) and only 280 mm $year^{-1}$ in the lower HRB in northwestern China (Si et al. 2005). It may therefore be deduced that *ET* from *T. ramosissima* stands is lower in its native regions than in regions it has invaded, but it remains unclear whether *T. ramosissima* stands have higher *ET* rates than other native species (e.g., *P. euphratica*).

In most previously published studies, the eddy covariance (EC) method has been widely used to estimate *ET* using direct measurements of latent heat fluxes (Sun et al. 2008). The objectives of this study were to determine the magnitude of *ET* for *P. euphratica* and *T. ramosissima* stands in the lower HRB, and compared them to other regions around the world. For this purpose, we gathered nearly 2 years of EC observations from two stands in the lower HRB. In addition, we concurrently observed meteorological variables and groundwater tables in the same plot used to determine environmental controls of *ET*.

Materials and methods

Study site

The climate in this region is extremely arid with a mean annual precipitation of only 37.4 mm, of which > 75% occurs between June and August. Annual pan evaporation is 3390.3 mm, which is greater than precipitation by a factor of 90. Mean annual temperatures in July and January are 27.0 and − 11.7 °C, respectively, as recorded at the Ejin meteorological station between 1959 and 2011 (Yu et al. 2013b). Mean values ± standard deviation (SD) of meteorological conditions for 2012 and 2014 are provided in Table 1. Given that both the highest rainfalls and temperatures occur concurrently in this region, most rainfall is depleted by evaporation before it infiltrates into the soil. Therefore, the effect of rainfall on the water balance is minimal. In addition to rainfall, groundwater recharged by runoff from the Heihe River sustains both local residents and regional ecosystems (Si et al. 2014).

We selected *T. ramosissima* and *P. euphratica* stands, two typical forest types in arid regions, to conduct EC measurements. The *T. ramosissima* stand (42°01′N, 101°03′E; 926 m a.s.l.) is situated in a north–south direction in the Alxa Desert Ecohydrology Experimental Research Station, Chinese Academy of Sciences. The *P. euphratica* stand (41°59′N, 101°10′E; 920 m AMSL) is located at the *P. euphratica* Forest National Nature Refuge at Qidaoqiao (Fig. 1). We initially conducted a comprehensive quadrat sampling of vegetation in 2010 for both forest types (Table 2). Leaf area index (LAI) of canopies was measured using a plant canopy analyzer (LAI-2200, LI-COR Biosciences, Inc., Lincoln, NE, USA) with one wand for both above- and below-canopy measurements

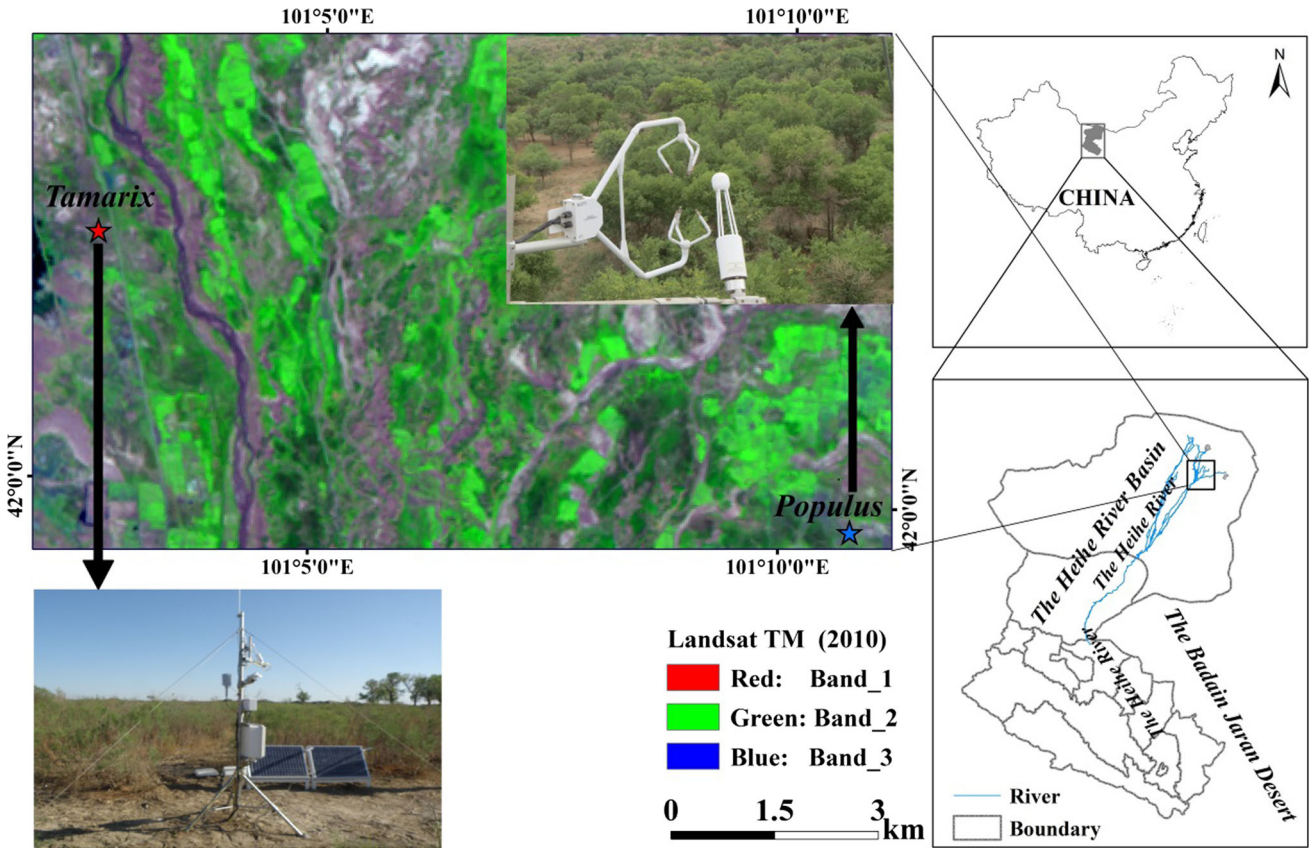

Fig. 1 Map of the Heihe River basin and the locations of the *T. ramosissima* and *P. euphratica* stands

Table 2 Statistical features of the *T. ramosissima* and *P. euphratica* stands

Stands	MA (years)	PD (ind. a^{-1})	MH (m)	MCA (m^2)	DBH (cm)	VC (%)	LAI_{max}
T. ramosissima	4	1300	1.87	5.11	2.05	52	1.97
P. euphratica	38	320	9.01	14.82	18.45	47	2.15

MA mean age, *PD* population density, *MH* mean height, *MCA*, mean crown area, *DBH* diameter at breast height, *VC* vegetation coverage, LAI_{max} maximum leaf area index

under diffused light conditions during sunrise and sunset. This was carried out approximately once every month throughout the growing season in both years. The understory was composed of shallow-rooted grasses, predominantly *Sophora alopecuroides* L., *Karelinia caspica* (Pall.) Less., and *Achnatherum splendens* (Trin.) Nevski. Soil characteristics from the *T. ramosissima* (Yu et al. 2013a) and *P. euphratica* stands were determined (Gao et al. 2016b).

Flux and meteorological measurements

Momentum flux, sensible heat (H, W m^{-2}), and latent heat (LE, W m^{-2}) were measured using a three-dimensional sonic anemometer (CSAT3, Campbell Scientific, Inc., North Logan, UT, USA) and an open path CO_2/H_2O analyzer (LI-7500A, LI-COR Biosciences, Inc., USA). In addition, meteorological variables were recorded, including net radiation (R_n, W m^{-2}), air temperature (T_a, °C), and relative humidity (RH, %) in conjunction with online-processed 0.5 h mean horizontal wind speeds (U, m s^{-1}) and CO_2/H_2O flux rates using the CR3000 datalogger (Campbell Scientific Inc., USA). R_n was determined using a four-component net radiometer (CNR4, Kipp & Zonen, Delft, the Netherlands), while T_a and RH were measured using a relative humidity and temperature sensor probe (HMP45C, Campbell Scientific, Inc, USA). The vapor pressure deficit (VPD, kPa) was calculated based on T_a and RH (Campbell and Norman 1998). Soil heat flux (G, W m^{-2}) was measured using a heat flux plate (HFP01, Hukseflux Thermal Sensors B.V., Delft, the Netherlands) at a 5 cm depth dispersed 0.5 m belowground horizontally.

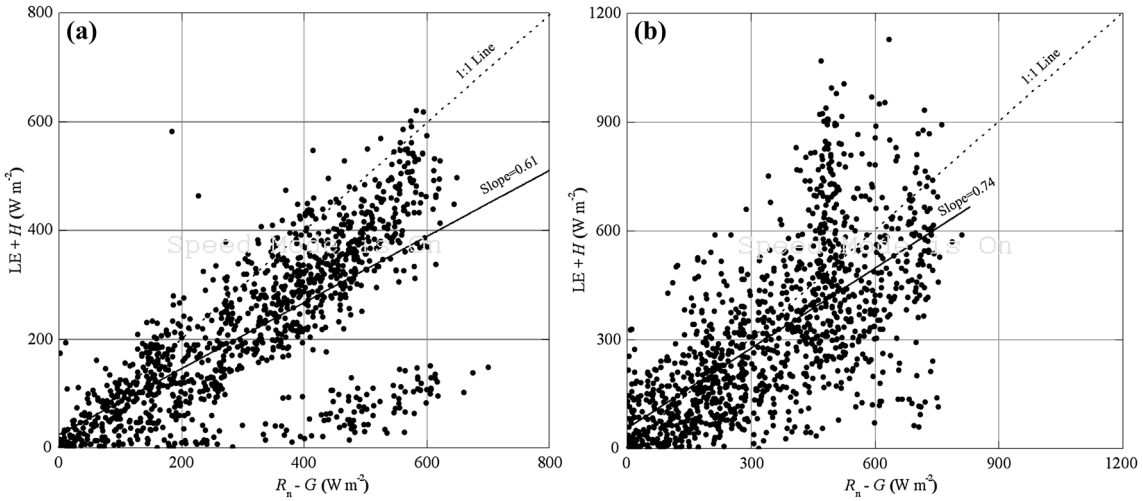

Fig. 2 Energy balance closures of eddy covariance (EC) for *T. ramosissima* (**a**) and *P. euphratica* (**b**) during 2012 and 2014, respectively. The 1:1 line (dotted line) and linear regression (solid line) between $R_n - G$ and $LE + H$ is shown

We conducted *T. ramosissima* stand flux and meteorological measurements from May 2011 to November 2012 at 3 m above-ground level. Subsequently, this method was applied to a 20 m high flux tower to measure *P. euphratica* stand flux and meteorological measurements from June 2013 to the present (Gao et al. 2016b). To compare, we selected the entire 2012 and 2014 growing seasons (i.e., from May to September) under similar meteorological conditions for analysis. In addition, two wells 30 m apart from the EC tower were installed and groundwater depth (*GD*, m) measured at 5 day intervals during the growing seasons, which provided results of a maximum of 2.65 m for the *T. ramosissima* stand and 2.25 m for the *P. euphratica* stand. Water was introduced via the Heihe River EWCP (set up to provide local herdsmen a means to irrigate their pastures) to the *P. euphratica* stand after September 16, 2014.

Data processing and gap filling

Raw CSAT3 and CO_2/H_2O flux data were processed using EddyPro software (LI-COR Biosciences, Inc., USA), which includes features such as double coordinate rotation, block average detrending, time lag compensation via covariance maximization (with defaults), and density fluctuation compensation via the use/convert features to the mixing ratio (Burba et al. 2012). Statistical analysis of the raw time series data was carried out, including spike count/removal, amplitude resolution, dropouts, absolute limits, and skewness and kurtosis, according to Vickers and Mahrt (1997). Quality checks/flagging were conducted according to the CarboEurope standard (Foken et al. 2004). After conducting a detailed postproduction on data, *H* and *LE* were calculated to obtain a 0.5 h average. We screened 0.5 h turbulent fluxes and meteorological variables to remove spurious data points caused by sensor malfunctions, rain events, and sensor maintenance.

The energy balance was analyzed from the EC data that include R_n, *LE*, and *H* and *G* calculated from the average of the two heat flux plate measurements. We disregarded canopy storage heat and photosynthetic energy consumption due to the sparseness of canopy cover. The relationship between the half-hourly data of net radiation subtracted by the ground heat flux ($R_n - G$) and the half-hourly data of the total turbulent flux ($LE + H$) indicated that EC underestimated turbulent fluxes by 22% (slope = 0.78; $R^2 = 0.91$) and 21% (slope = 0.79; $R^2 = 0.80$) for the *T. ramosissima* and *P. euphratica* stands, respectively (Fig. 2). *LE* data was also removed from the energy unbalance. In total, 34 and 19% of the original *LE* data was rejected during data quality processing of the *T. ramosissima* and *P. euphratica* stands, respectively.

Gap filling was carried out when total *ET* had to be calculated by filling shorter gaps (i.e., < 2 h) in the data through linear interpolation, and longer gaps in *LE* flux using energy balance analysis. If EC measured *LE* was greater than $R_n + G - H$ or null, we then forced *LE* to close according to the energy balance analysis (Yuan et al. 2014), that is, $LE = R_n + G - H$, otherwise *LE* was retained. *ET* (mm h^{-1}) from *LE* was calculated hourly according to Yuan et al. (2014), the actual *ET* (mm h^{-1}) from combined data with EC measured *ET* (ET_{EC}, mm h^{-1}), and the estimated *ET* from the energy balance analysis (ET_{EB}, mm h^{-1}) (Fig. 3). When hourly *ET* was negative, it was set to zero. Daily *ET* (mm day^{-1}) was the sum of hourly *ET* during a single day. In addition, the daily reference *ET* (ET_0, mm day^{-1}) was calculated from the FAO Penman–Monteith equation (Allen et al. 1998) on a

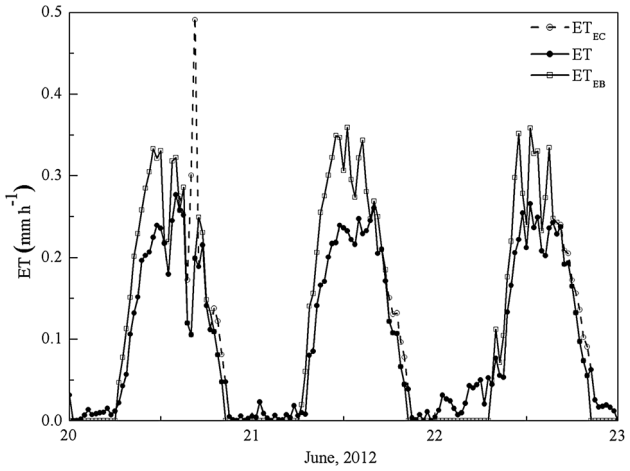

Fig. 3 Hourly variation in measured evapotranspiration from eddy covariance (EC) (ET_{EC}, mm h^{-1}), estimated evapotranspiration derived from energy balance analysis (ET_{EB}, mm h^{-1}), and actual evapotranspiration calculated from the combination of the two (*ET*, mm h^{-1}) for the *T. ramosissima* stand from June 20 to June 23, 2012

daily scale. R_n and *G* data were used to calculate daily ET_0 derived from observations from flux tower measurements, and other daily data from the Ejin meteorological station. The crop coefficient ($K_c = ET/ET_0$) was then determined.

Data analysis

Basic statistical features of mean values and SD for meteorological variables were analyzed and significant differences tested using one-way ANOVA at $P = 0.05$. Meteorological data collected from the site were used, including R_n, T_a, *RH*, *U*, and *VPD*, to explain seasonal *ET* variability by ANOVA as well as correlation and regression analyses provided in the SPSS Statistics 19 software package (IBM, USA). Finally, Origin 8.0 software was used to generate drawings (OriginLab Corp., Northampton, MA, USA).

Results

Comparisons of environmental variables

Limited precipitation, low *RH* as well as high T_a and *VPD* were the main climatic variables used for the study area. Precipitation was 32.7 mm in 2012 and 17.2 mm in 2014. Two extreme precipitation events, 8.3 and 8.9 mm on June 6 and July 24, respectively, could account for the high precipitation in 2012. At $P = 0.05$, population means of *N*, T_a, *VPD*, and *U* were not significantly different for either study year with the exception of *RH* from the meteorological station (Table 1).

For the *T. ramosissima* stand, daily R_n increased during the spring and progressed into the summer before progressively decreasing during the autumn from 3.0 to 21.0 MJ m^{-2} day^{-1} with an average of 12.4 MJ m^{-2} day^{-1}. Moreover, *G* was coincident with R_n (Fig. 4a). Daily T_a remained positive at an average of 18.5 °C throughout the growing seasons, particularly in August when maximum daily T_a reached 31.6 °C. Seasonal variation in *RH* changed following R_n and T_a with an average of 31.3% (Fig. 4b) and was particularly low from March to May compared to other months (20.2 vs. 35.9%, $P = 0.01$), which may be attributable to the high *U* observed during this period (2.1 vs. 1.4 m s^{-1}, $P = 0.05$) (Fig. 4c). Mean *VPD* was 1.8 kPa, and seasonal variation in *VPD* was closely correlated to R_n and T_a (Fig. 4c).

For the *P. euphratica* stand, R_n was significantly higher with an average of 14.1 MJ m^{-2} day^{-1} compared to the *T. ramosissima* stand ($P = 0.01$) during the growing seasons, and *G* coincided with R_n (Fig. 4d). T_a and *RH*, with an average of 19.0 °C and 29.1%, was not significantly different from the *T. ramosissima* stand ($P = 0.50$ and $P = 0.07$, respectively) (Fig. 4e). Undifferentiated T_a and *RH* resulting from *VPD* was also not significantly different (1.8 kPa, $P = 0.75$) to the *T. ramosissima* stand (Fig. 4f). Height (20 m) of measured *U* results was significantly higher (3.4 vs. 1.6 m s^{-1}, $P = 0.01$) compared to the *T. ramosissima* stand.

Comparison of evapotranspiration between the two stands

Energy balance closures $(LE + H)/(R_n - G)$ were 79 and 78% in 2012 and 2014, respectively (Fig. 2). During the dormant season, daily *ET* was generally less than 0.5 mm day^{-1}. It is noteworthy that *ET* remained weak throughout March and April but ET_0 remained relatively high (Fig. 5a), from which T_a, *VPD*, and *U* increased rapidly (Fig. 4b, c). For the growing season, daily *ET* increased during the spring and progressed into the summer before progressively decreasing in the autumn from 0.3 to 8.0 mm day^{-1} with an average of 3.6 mm day^{-1} (Fig. 5a). However, there was pronounced lower *ET* value in June that was consistent with the lower *U* for the same period, although it rose sharply afterwards in conjunction with the high *VPD* in August with a maximum of 7.7 mm day^{-1}. In contrast, ET_0 was high during the late spring and autumn, indicating a low *ET* to ET_0 ratio (K_c: from 0.09 to 0.22) during these periods. In comparison, K_c remained high (0.36–0.86) during the summer and early autumn with an average of 0.46 in 2012. This phenomenon indicated that soil evaporation was weak because plant transpiration could not have occurred in March and April. Monthly *ET* increased from 34.1 mm in May to 180.1 mm in July and decreased to 93.1 mm in September for a total of 548 mm in 2012 (Table 3).

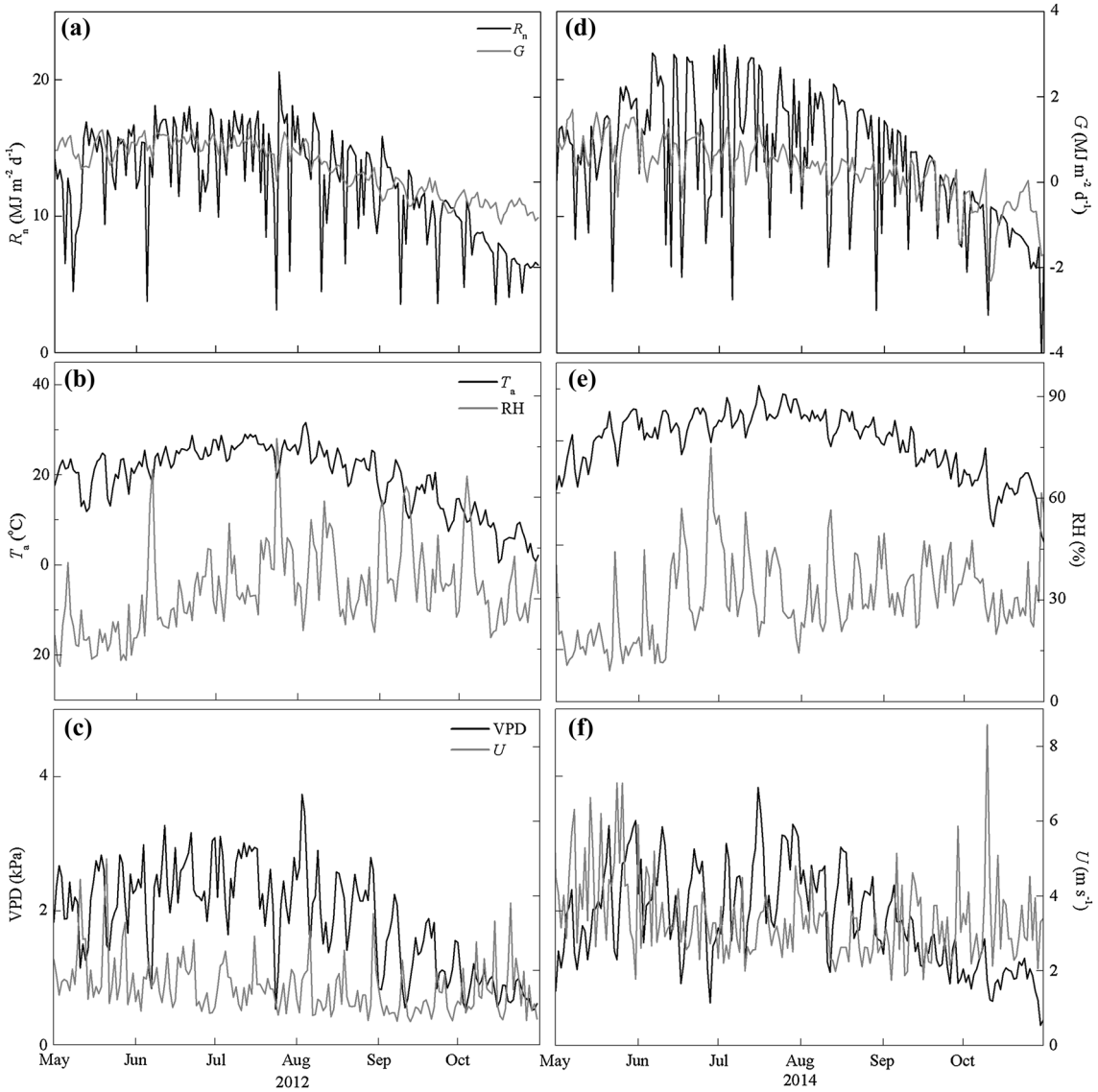

Fig. 4 Daily variation in meteorological variables, including net radiation (R_n, W m^{-2}), soil heat flux (G, W m^{-2}), air temperature (T_a, °C), relative humidity (*RH*, %), vapor pressure deficit (*VPD*, kPa), and wind speed (U, m s^{-1}) for *T. ramosissima* (**a**–**c**) and *P. euphratica* (**d**–**f**) during 2012 and 2014 growing seasons

For the *P. euphratica* stand, *ET* increased earlier and ended later than for the *T. ramosissima* stand, after which it was consistent with ET_0 (Fig. 5b). Daily *ET* was less than 1 mm prior to March ($T_a < 0$ °C) during the dormant season (Fig. 5b). However, *ET* increased rapidly with a peak of 3 mm day^{-1} after March, at which time T_a, *VPD* and U increased rapidly (Fig. 4e and f), and ET_0 was relatively high (Fig. 5b). During the growing season, daily *ET* ranged from 0.9 to 7.9 mm with an average of 4.6 mm day^{-1} (Fig. 5b), and monthly *ET* increased from 131.3 mm in May to 170.0 mm in July and decreased to 98.5 mm in September for a total of 707 mm in 2014 (Table 3).

Comparison of variables associated with evapotranspiration

For the *T. ramosissima* stand, daily *ET* was positive and significantly correlated to R_n, T_a, and *VPD* and negative and significantly correlated to *RH*, but not significantly correlated to U. Due to the high correlations between *VPD* and *RH*, the latter was removed during stepwise regression analysis, for which the results revealed that climate variables accounted for at least 81% of *ET* variation. For the *P. euphratica* stand, daily *ET* also positive and significantly correlated to R_n, T_a, and *VPD* and negative and significantly correlated to *RH* (U being the exception), and climate factors, including R_n, T_a, and *VPD*, accounted for at least 80% of *ET* variation (Table 4).

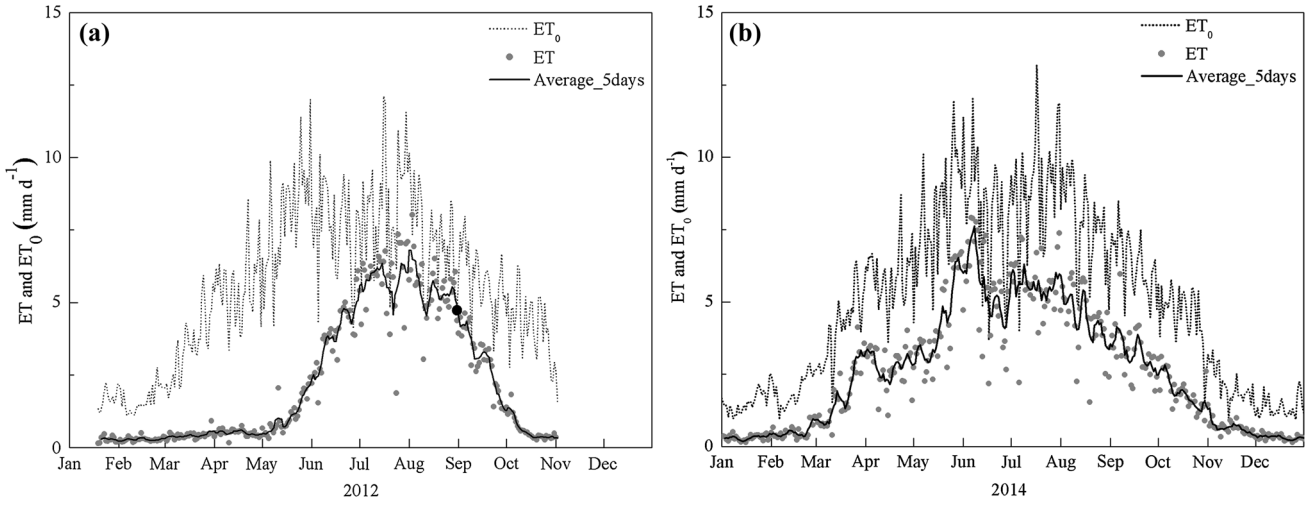

Fig. 5 Seasonal patterns in daily reference evapotranspiration (ET_0, mm day^{-1}) and evapotranspiration (ET, mm day^{-1}) for *T. ramosissima* (**a**) and *P. euphratica* (**b**) in 2012 and 2014. The 5-day average value of ET (black solid line) is shown

Table 3 Monthly variation in evapotranspiration (ET, mm), reference evapotranspiration (ET_0, mm), and crop coefficient ($K_c = ET/ET_0$) of *T. ramosissima* and *P. euphratica* during the 2012 and 2014 growing seasons

Years	May	June	July	Aug.	Sept.	Total
2012						
ET						
Mean	1.1*	3.9*	4.4*	5.4*	3.0	3.6*
Sum	34.6	117.5	136.4	166.8	93.1	548.4
ET0						
Mean	8.0	7.6	8.4	7.2	5.8	6.6
Sum	247.3	227.3	259.9	222.0	173.9	1261.3
K_c	0.14	0.51	0.69	0.77	0.52	0.48
2014						
ET						
Mean	4.2*	5.5*	5.6*	4.4*	3.3	4.6*
Sum	131.3	165.5	175.0	137.0	98.5	707.3
ET0						
Mean	7.4	7.4	7.9	7.1	5.8	6.9
Sum	230.4	221.0	245.2	218.9	175.3	1218.1
K_c	0.57	0.75	0.71	0.63	0.56	0.63

* Significant differences in mean evapotranspiration for months and years were tested using one-way ANOVA at $P = 0.05$

Table 4 Statistical summary of evapotranspiration patterns (dependent variables) to climate parameters for *T. ramosissima* and *P. euphratica* during the 2012 and 2014 growing seasons

Years	Correlation analysis					Regression analysis		
	R_n	T_a	*RH*	*VPD*	*U*	Model parameters	*F*	R^2
2012	0.58	0.75	− 0.26	0.60	n. s.	R_n, T_a, VPD	114	0.81
2014	0.82	0.75	− 0.21	0.75	n. s.	R_n, T_a, VPD	241	0.80

Pearson correlation coefficients and stepwise regressions were considered significant at $P = 0.01$

Discussion

Comparison of evapotranspiration between the two stands

Energy balance closures for the two stands (Fig. 2) were comparable with FLUXNET sites (Wilson et al. 2002) as well as with other EC measurements, especially in the arid region of northwestern China (Hao et al. 2007; Yuan et al. 2014). This suggests that direct *ET* measurements using the EC method were reliable. The total *ET* of *T. ramosissima* and *P. euphratica* during the growing season has been estimated at tree-level (Si et al. 2007; Zhang et al. 2006) and stand-level scales (Hou et al. 2010; Si et al. 2005; Wang et al. 2014). The BREB estimated *ET* was approximately 248 mm with an average of 1.6 mm day^{-1} for *T. ramosissima* (Si et al. 2005) and 447 mm with an average of 3.2 mm day^{-1} for the *P. euphratica* stand (Hou et al. 2010). In addition, annual transpiration measured through sap flow was 214.9 mm for *P. euphratica* (Si et al. 2007). The daily ET rate during the summer months (June–August) was estimated to be 0.63–0.73 mm for *T. ramosissima* and 1.89–2.33 mm for *P. euphratica* using the water table fluctuation (WTF) method (Wang et al. 2014). A comparison of results from this study and those of the aforementioned studies indicate that the *ET* rates estimated using the EC method for both stands were higher than values determined through sap flow, BREB, and WTF methods.

Previous studies (Cleverly et al. 2006; Devitt et al. 2011) have shown that climate factors, vegetation parameters, soil properties, and water table depths are principal factors controlling *ET* variation in phreatophytic communities. Climate variables, soil types, plant community composition, and water table depth for the two stands were similar for both years (Tables 1, 2). Thus, their different *ET* values were likely caused by differing soil moisture levels induced by irrigation and further different soil evaporative conditions (Fig. 5). Before 2013, the *P. euphratica* stand had no access to irrigation and groundwater depth may have been 4 m. After 2013, the irrigation was applied in autumn. Thus, we deduced that the significantly higher *ET* found in the *P. euphratica* stand was directly related to the high soil evaporation rate at this site. Reasons for this are discussed below.

Comparison of evapotranspiration between the study sites to other regions

Due to its wide distribution, *ET* from *Tamarix* species, an introduced, stress-tolerant shrub from Central Asia, has been extensively investigated throughout the world. The *ET* results from the *T. ramosissima* stand using EC were similar to results in the lower Tarim River basin, China, with a mean *ET* of 500 mm a^{-1} and an average *ET* of 3.85 mm day^{-1} (Yuan et al. 2014). A comparison of results obtained from this study and one in the lower Tarim River (Yuan et al. 2014) showed that *T. ramosissima* growth in both did not experience water stress. Thus, results from both studies may represent potential *ET* for native *T. ramosissima* stands in Central Asia. It is noteworthy that the slightly higher *ET* found in our study (compared to the results of Yuan et al. 2014) may be attributed to the relatively higher LAI (1.97 vs. 1.15, respectively) and the lower groundwater depth (2.65 vs. 6.62 m, respectively).

However, total *ET* obtained from EC flux tower measurements (Cleverly et al. 2002, 2006; Devitt et al. 1998; Westenburg et al. 2006) in combination with remote sensing data (Bawazir et al. 2009; Nagler et al. 2005, 2009; Taghvaeian et al. 2014) yielded a broad range from 800 to 1450 mm $year^{-1}$ in the western United States. It may therefore be concluded that observed *ET* under arid conditions in native regions was clearly low compared to invasive *T. ramosissima* stands in non-native regions. These differences could be attributable to two specific reasons. First, soil evaporation in *T. ramosissima* stands in arid regions could be either weak or negligible (Yuan et al. 2014). Second, although LAI can have a deterministic impact on total *ET* (Dahm et al. 2002; Sala et al. 1996; Yuan et al. 2014), values from the study and those of Yuan et al. (2014) were lower than those in the middle Rio Grande district (2.5 and 3.5 for flooding and non-flooding, respectively) (Cleverly et al. 2006; Nagler et al. 2005) and the lower Colorado River (2.54) (Nagler et al. 2009), both in the western U.S.

Recent studies have shown that water use by individual *T. ramosissima* trees is comparable to the native species that it typically replaces such as cottonwood and willow (Glenn and Nagler 2005; Nagler et al. 2003). However, in these cases tree-level soil evaporation had not been taken into account. Although soil evaporation was weak for the *T. ramosissima* stand as reported by Yuan et al. (2014), this was not the case for the *P. euphratica* stand due to the high *ET* observed during the dormant season (Fig. 5b). Based on the simplified Shuttleworth–Wallace (SSW) model, the ratio of canopy transpiration to *ET* ranged from 0.53 to 0.66 (Gao et al. 2016a). Thus, we estimated that transpiration was 465 mm for the *P. euphratica* stand which was comparable to 473 mm for the *T. ramosissima* stand when soil evaporation was disregarded (a total of 77 mm a^{-1} with an average of 0.5 mm day^{-1} determined by measuring *ET* during the dormant season in conjunction with results from Yuan et al. (2014). For greater accuracy, further research is required to partition *ET* into plant transpiration and soil evaporation.

Factors and variables associated with evapotranspiration

ET rates responded to *GD*, atmospheric surface layer conditions, stomatal coupling in conjunction with atmospheric humidity levels, energy balances, and LAI (Cleverly et al. 2006). In desert riparian regions, given the limited rainfall, groundwater provides an ample water supply to riparian forests (Si et al. 2014), permitting greater annual *ET* rates than that provided by rainfall alone (Table 3). Some studies have shown that growth and eco-physiological parameters of riparian forests were less severely affected by *GD* within a depth of 6 m in arid regions in China (Chen et al. 2006; Feng et al. 2012; Hao et al. 2009). Measured *ET* of *T. ramosissima* and *P. euphratica* stands using the EC method in the lower HRB was comparable to results in the Tarim River basin (Yuan et al. 2014). In contrast, the clear differences in *ET* in native and invasive regions indicate that climate factors and water availability, which both impact plant eco-physiological characteristics, were the primary controllers of water use for these species.

Regression analysis demonstrate that climate and soil water variables accounting for at least 80% of *ET* variation in the two riparian forests investigated (Table 4). In addition, plant eco-physiological characteristics, particularly LAI, determined spatial patterns of *ET* for riparian phreatophytes. Moreover, LAI in combination with plant physiological parameters such as stomatal conductance, would impact seasonal variation in *ET* (Hatler and Hart 2009). Desert riparian species adapted to arid climates may use of deep soil water and groundwater at the same time. In contrast, greater amounts of rainfall and flooding may supply sufficient available water in shallow soil layers of the arid southwestern U.S. This suggests that plant water use is the result of long-term adaption to local climates and water availability.

Conclusions

During the growing season, *ET* of the *T. ramosissima* stand was 548 mm a^{-1} with a mean of 3.6 mm day^{-1}, similar to that of native forests in Central Asia (500 mm a^{-1}) but clearly lower than that of invasive regions in the western U.S. (from 800 to 1450 mm a^{-1}). *ET* of the *P. euphratica* stand was 707 mm with a mean of 4.6 mm day^{-1}, which was directly linked to high soil evaporation rates under sufficient water availability induced by irrigation. When soil evaporation was disregarded, total transpiration was 473 and 465 mm for the *P. euphratica* and *T. ramosissima* stands, respectively, indicating comparable water use of the two contrasting riparian forests. Furthermore, regression analysis demonstrated that climate factors accounted for at least 80% of *ET* variation for both stands. Thus, our results show that plant water use is the result of long-term adaptation to local climates and water availability.

Acknowledgements The authors would like to thank two anonymous reviewers for their constructive and valuable assessment and comments, which helped to improve this article.

References

Allen R, Pereira LS, Raes D, Smith M (1998) Crop evapotranspiration-guidelines for computing crop requirements. In: FAO irrigation and drainage paper 56. FAO, Rome

Bawazir AS, Samani Z, Bleiweiss M, Skaggs R, Schmugge T (2009) Using ASTER satellite data to calculate riparian evapotranspiration in the Middle Rio Grande, New Mexico. Int J Remote Sens 30:5593–5603

Burba G, Schmidt A, Scott RL, Nakai T, Kathilankal J, Fratini G, Hanson C, Law B, McDermitt DK, Eckles R, Furtaw M, Velgersdyk M (2012) Calculating CO_2 and H_2O eddy covariance fluxes from an enclosed gas analyzer using an instantaneous mixing ratio. Glob Change Biol 18:385–399

Campbell GS, Norman JM (1998) An introduction to environmental biophysics. Springer-Verlag New York Inc, New York

Chen YN, Wang Q, Li W, Ruan X, Chen Y, Zhang L (2006) Rational groundwater table indicated by the eco-physiological parameters of the vegetation: a case study of ecological restoration in the lower reaches of the Tarim River. Chin Sci Bull 51:8–15

Cheng GD, Li X, Zhao WZ, Xu ZM, Feng Q, Xiao SC, Xiao HL (2014) Integrated study of the water-ecosystem-economy in the Heihe River basin. Natl Sci Rev 1:413–428

Cleverly JR, Dahm CN, Thibault JR, Gilroy DJ, Allred Coonrod JE (2002) Seasonal estimates of actual evapo-transpiration from *Tamarix ramosissima* stands using three-dimensional eddy covariance. J Arid Environ 52:181–197

Cleverly JR, Dahm CN, Thibault JR, McDonnell DE, Allred Coonrod JE (2006) Riparian ecohydrology: regulation of water flux from the ground to the atmosphere in the Middle Rio Grande, New Mexico. Hydrol Process 20:3207–3225

Dahm CN, Cleverly JR, Allred Coonrod JE, Thibault JR, McDonnell DE, Gilroy DJ (2002) Evapotranspiration at the land/water interface in a semi-arid drainage basin. Freshw Biol 47:831–843

Dennison PE, Nagler PL, Hultine KR, Glenn EP, Ehleringer JR (2009) Remote monitoring of tamarisk defoliation and evapotranspiration following saltcedar leaf beetle attack. Remote Sens Environ 113:1462–1472

Devitt DA, Sala A, Smith SD, Cleverly J, Shaulis LK, Hammett R (1998) Bowen ratio estimates of evapotranspiration for *Tamarix ramosissima* stands on the Virgin River in southern Nevada. Water Resour Res 34:2407–2414

Devitt DA, Fenstermaker LF, Young MH, Conrad B, Baghzouz M, Bird BM (2011) Evapotranspiration of mixed shrub communities in phreatophytic zones of the Great Basin region of Nevada (USA). Ecohydrology 4:807–822

Di Tomaso JM (1998) Impact, biology, and ecology of Saltcedar (*Tamarix* spp.) in the southwestern United States. Weed Technol 12:326–336

Feng Q, Cheng GD (1998) Current situation, problems and rational utilization of water resources in arid north-western China. J Arid Environ 40:373–382

Feng Q, Peng JZ, Li J, Xi HY, Si JH (2012) Using the concept of ecological groundwater level to evaluate shallow groundwater resources in hyperarid desert regions. J Arid Land 4:378–389

Foken T, Gockede M, Mauder M, Mahrt L, Amiro B, Munger W (2004) Post-field data quality control. In: Xuhui L, William M, Beverly L (eds) Handbook of micrometeorology: a guide for surface flux measurements. Kluwer Academic Publishers, New York, pp 181–203

Gao GL, Zhang XY, Yu TF, Liu B (2016a) Comparison of three evapotranspiration models with eddy covariance measurements for a *Populus euphratica* Oliv. forest in an arid region of northwestern China. J Arid Land 8:146–156

Gao GL, Zhang XY, Yu TF (2016b) Evapotranspiration of a *Populus euphratica* forest during the growing season in an extremely arid region of northwest China using the shuttleworth-wallace model. J For Res 27:879–887

Glenn EP, Nagler PL (2005) Comparative ecophysiology of *Tamarix ramosissima* and native trees in western U.S. riparian zones. J Arid Environ 61:419–446

Guo QL, Feng Q, Li JL (2008) Environmental changes after ecological water conveyance in the lower reaches of Heihe River, northwest China. Environ Geol 58:1387–1396

Hao YB, Wang Y, Huang X, Cui X, Zhou X, Wang S, Niu H, Jiang G (2007) Seasonal and interannual variation in water vapor and energy exchange over a typical steppe in Inner Mongolia, China. Agric For Meteorol 146:57–69

Hao XM, Li WH, Huang X, Zhu C, Ma J (2009) Assessment of the groundwater threshold of desert riparian forest vegetation along the middle and lower reaches of the Tarim River, China. Hydrol Process 24:178–186

Hatler WL, Hart CR (2009) Water loss and salvage in saltcedar (*Tamarix* spp.) stands on the Pecos River, Texas. Invasive Plant Sci Manag 2:309–317

Hou LG, Xiao HL, Si JH, Xiao SC, Zhou MX, Yang YG (2010) Evapotranspiration and crop coefficient of *Populus euphratica* Oliv forest during the growing season in the extreme arid region northwest China. Agric Water Manag 97:351–356

Nagler PL, Glenn EP, Lewis Thompson T (2003) Comparison of transpiration rates among saltcedar, cottonwood and willow trees by sap flow and canopy temperature methods. Agric For Meteorol 116:73–89

Nagler P, Scott R, Westenburg C, Cleverly J, Glenn E, Huete A (2005) Evapotranspiration on western U.S. rivers estimated using the Enhanced Vegetation Index from MODIS and data from eddy covariance and Bowen ratio flux towers. Remote Sens Environ 97:337–351

Nagler PL, Morino K, Didan K, Erker J, Osterberg J, Hultine KR, Glenn EP (2009) Wide-area estimates of saltcedar (Tamarix spp.) evapotranspiration on the lower Colorado River measured by heat balance and remote sensing methods. Ecohydrology 2:18–33

Sala A, Smith SD, Devitt DA (1996) Water use by *Tamarix ramosissima* and associated phreatophytes in a Mojave Desert floodplain. Ecol Appl 6:888–898

Shafroth PB, Cleverly JR, Dudley TL, Taylor JP, van Riper C III, Weeks EP, Stuart JN (2005) Control of Tamarix in the Western United States: implications for water salvage, wildlife use, and riparian restoration. Environ Manag 35:231–246

Si JH, Feng Q, Zhang XY, Liu W, Su YH, Zhang YW (2005) Growing season evapotranspiration from *Tamarix ramosissima* stands under extreme arid conditions in northwest China. Environ Geol 48:861–870

Si JH, Feng Q, Zhang XY, Chang ZQ, Su YH, Xi HY (2007) Sap flow of *Populus euphratica* in a desert riparian forest in an extreme arid region during the growing season. J Integr Plant Biol 49:425–436

Si JH, Feng Q, Cao SK, Yu TF, Zhao CY (2014) Water use sources of desert riparian *Populus euphratica* forests. Environ Monit Assess 186:5469–5477

Smith SD, Devitt DA, Sala A, Cleverly JR, Busch DE (1998) Water relations of riparian plants from warm desert regions. Wetlands 18:687–696

Sun G, Noormets A, Chen J, McNulty SG (2008) Evapotranspiration estimates from eddy covariance towers and hydrologic modeling in managed forests in Northern Wisconsin, USA. Agric For Meteorol 148:257–267

Taghvaeian S, Neale CMU, Osterberg J, Sritharan SI, Watts DR (2014) Water use and stream-aquifer-phreatophyte interaction along a Tamarisk-dominated segment of the lower Colorado River. Remote Sens Terr Water Cycle, Geophysical Monograph 206, pp 95–113

Vickers D, Mahrt L (1997) Quality control and flux sampling problems for tower and aircraft data. J Atmos Ocean Technol 14:512–526

Wang P, Grinevsky SO, Pozdniakov SP, Yu JJ, Dautova DS, Min L, Du C, Zhang Y (2014) Application of the water table fluctuation method for estimating evapotranspiration at two phreatophyte-dominated sites under hyper-arid environments. J Hydrol 519:2289–2300

Westenburg CL, Harper DP, DeMeo GA (2006) Evapotranspiration by phreatophytes along the lower Colorado River at Havasu National Wildlife Refuge, Arizona. In: Geological survey scientific investigations report 2006-5043. Henderson

Wilson K, Goldstein A, Falge E, Aubinet M, Baldocchi D, Berbigier P, Bernhofer C, Ceulemans R, Dolman H, Field C, Grelle A, Ibrom A, Law BE, Kowalski A, Meyers T, Moncrieff J, Monson R, Oechel W, Tenhunen J, Valentini R, Verma S (2002) Energy balance closure at FLUXNET sites. Agric For Meteorol 113:223–243

Yu TF, Feng Q, Si JH, Xi HY, Li W (2013a) Patterns, magnitude, and controlling factors of hydraulic redistribution of soil water by *Tamarix ramosissima* roots. J Arid Land 5:396–407

Yu TF, Feng Q, Si JH, Xi HY, Li ZX, Chen AF (2013b) Hydraulic redistribution of soil water by roots of two desert riparian phreatophytes in northwest China's extremely arid region. Plant Soil 372:297–308

Yuan GF, Zhang P, Shao MA, Luo Y, Zhu XC (2014) Energy and water exchanges over a riparian *Tamarix* spp. stand in the lower Tarim River basin under a hyper-arid climate. Agric For Meteorol 194:144–154

Zhang XY, Kang ES, Si JH, Zhou MX (2006) Stem sap flow of individual plant of *Populus euphratica* and its conversion to forest water consumption. Scientia Silvae Sinicae 42:28–32